BNL-103653-2014-TECH
AGS/RHIC/SN 027;BNL-103653-2014-IR

# A Pion Polarimeter using Eight Toroidal Magnets

F. G. Mariam

May 1996

Collider Accelerator Department
**Brookhaven National Laboratory**

**U.S. Department of Energy**
USDOE Office of Science (SC)

# DISCLAIMER

Alternating Gradient Synchrotron Department
Relativistic Heavy Ion Collider Project
BROOKHAVEN NATIONAL LABORATORY

**Spin Note**

**AGS/RHIC/SN No. 027**
(May 2, 1996)

# A PION POLARIMETER USING EIGHT TOROIDAL MAGNETS

Fesseha G. Mariam

May 2, 1996

# A PION POLARIMETER USING EIGHT TOROIDAL MAGNETS

**Fesseha G. Mariam**
**Brookhaven National Laboratory**

A two-arm pion polarimeter utilizing toroidal magnets is being considered for use with the polarized proton beam at RHIC[1]. The underlying physics is based on experimental observations that showed significant analyzing power in pions produced by the interaction of high energy polarized proton with fixed targets[2,3]. The question of whether this polarimeter can be used to measure the absolute polarization of the RHIC beam is yet to be determined. Nonetheless, it can be used to measure the relative polarization, and as such is a necessary diagnostic tool for tuning the RHIC snake magnets and other polarization controlling elements.

This note addresses the polarimeter layout within the constraints of the q4 to q3 straight section of the RHIC lattice. A plausible magnet design based on TOSCA simulations is discussed and specification of the required power supplies is included. Preliminary estimates of acceptance and event rates are also given. Future and ongoing plans for further investigation are suggested in the summary. This note may also serve as a starting point from which one may further develop the hardware and optimize the system.

## 1. Proposed Layout and Magnets

Fig. 1 shows the proposed layout. Pions are produced by the interaction of polarized protons on a 5 micron carbon fiber about 1.5 meters downstream of q4. A string of eight toroids surrounds the warm beam line section between q4 and q3. The first toroid is 2 m long and the rest are 1.5 m long with inter-magnet drift of 0.6 meters (for possible placement of tracking detectors). This arrangement leaves ample space for a collimator and a 6 m long Cerenkov counter. It also fits in the space between the two RHIC rings.

The scheme calls for appropriate magnet settings so that pions of momenta between 12.5 GeV/c and 125 GeV/c at $p_T$=0.8 GeV/c can be guided through a collimator onto a common Cerenkov counter. The lower and higher momenta correspond to $x_F$=0.5 at the injection energy of $p_{beam}$=25 GeV/c and the top energy of $p_{beam}$=250 GeV/c, respectively. Even though it may be possible to accommodate other momenta ranges, we restrict our attention to pions with $x_F$=0.5 and $p_T$=0.8 GeV/c.

Each toroid consists of four pie-shaped pole pieces with a $7^\circ$ angular opening between adjacent poles (see fig. 2). Tracking detectors will determine the momenta of the particles accepted within the $7^\circ$ opening. The Cerenkov counter, operating either in the threshold or differential mode, will be used for particle identification. The details of the

[1] The original idea of using toroidal magnets for pion polarimetry is due to Dave Underwood.
[2] H. Spinka, et al, NIM 211 (1983) p. 239.
[3] D.L. Adams, et al, Phys. Rev. Lett. B, Vol. 264, No. 3.4, (1991) p. 462.

layout in fig. 1 are listed in table 2. For these simulations, the trajectories were calculated using the two-dimensional field map in the middle of the magnet. The magnets were assumed hard edged, i.e. fringe fields were ignored.

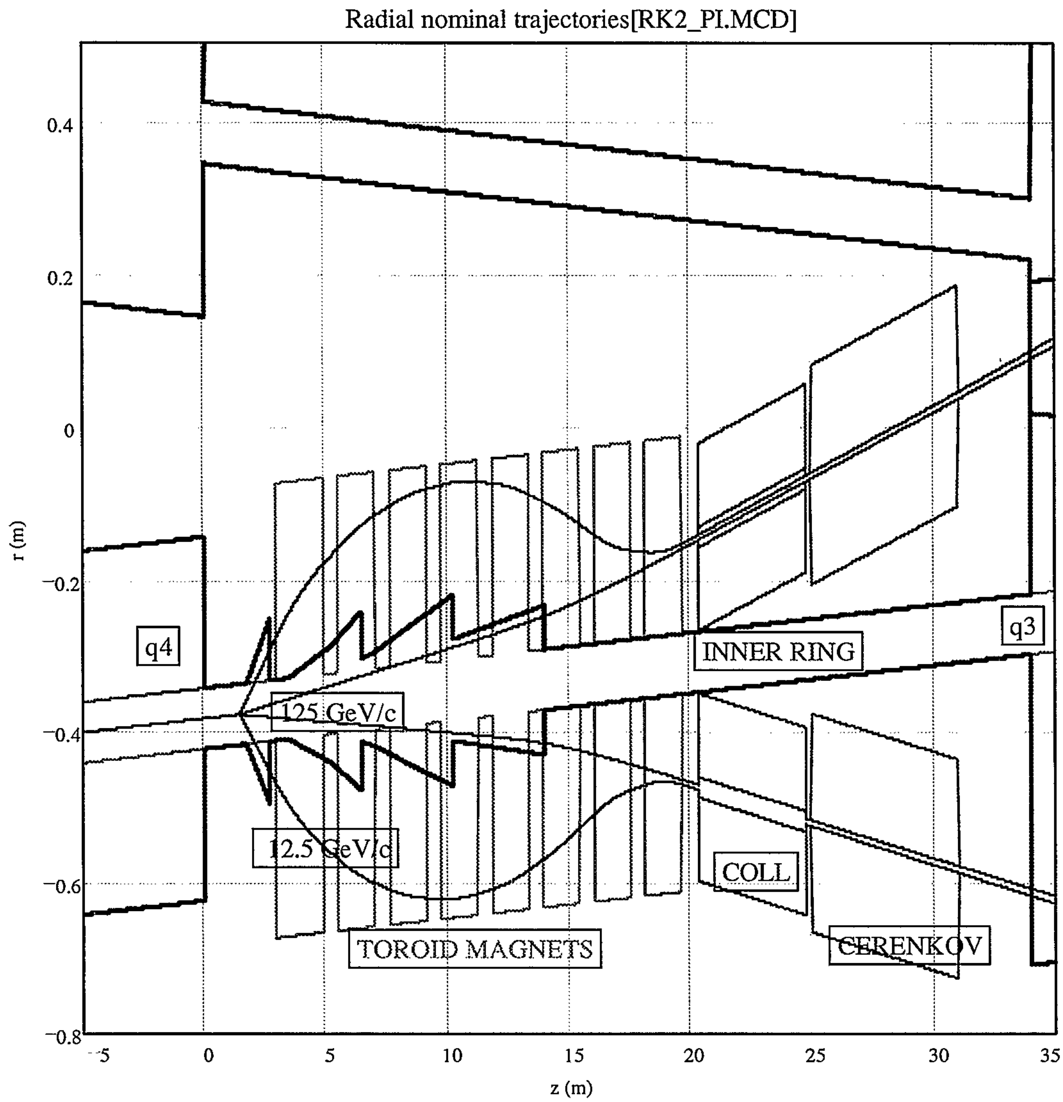


Fig. 1. Plan view of two-arm polarimeter using eight toroidal magnets between q4 and q3. The sections of the two RHIC rings between q4 and q3 are shown, including exit windows on the beam pipe surrounded by the toroids. Downstream of the magnets, the particles pass through a 2 cm slit collimator and onto a 6 m Cerenkov counter. Hardware and trajectories are drawn to scale. The field settings for the low and high energy trajectories indicated are given in table 2.

TOSCA designs of the toroidal magnets were performed by Masahiro Okamura. Several options were considered and the parameters of a suitable design are indicated in fig. 2 while a preliminary specification of the power requirements are given in table 1. Bipolar power supplies are necessary for measurements with positive as well as negative pions and for flexibility in tuning. The original RHIC specification calls for a 13 cm beam

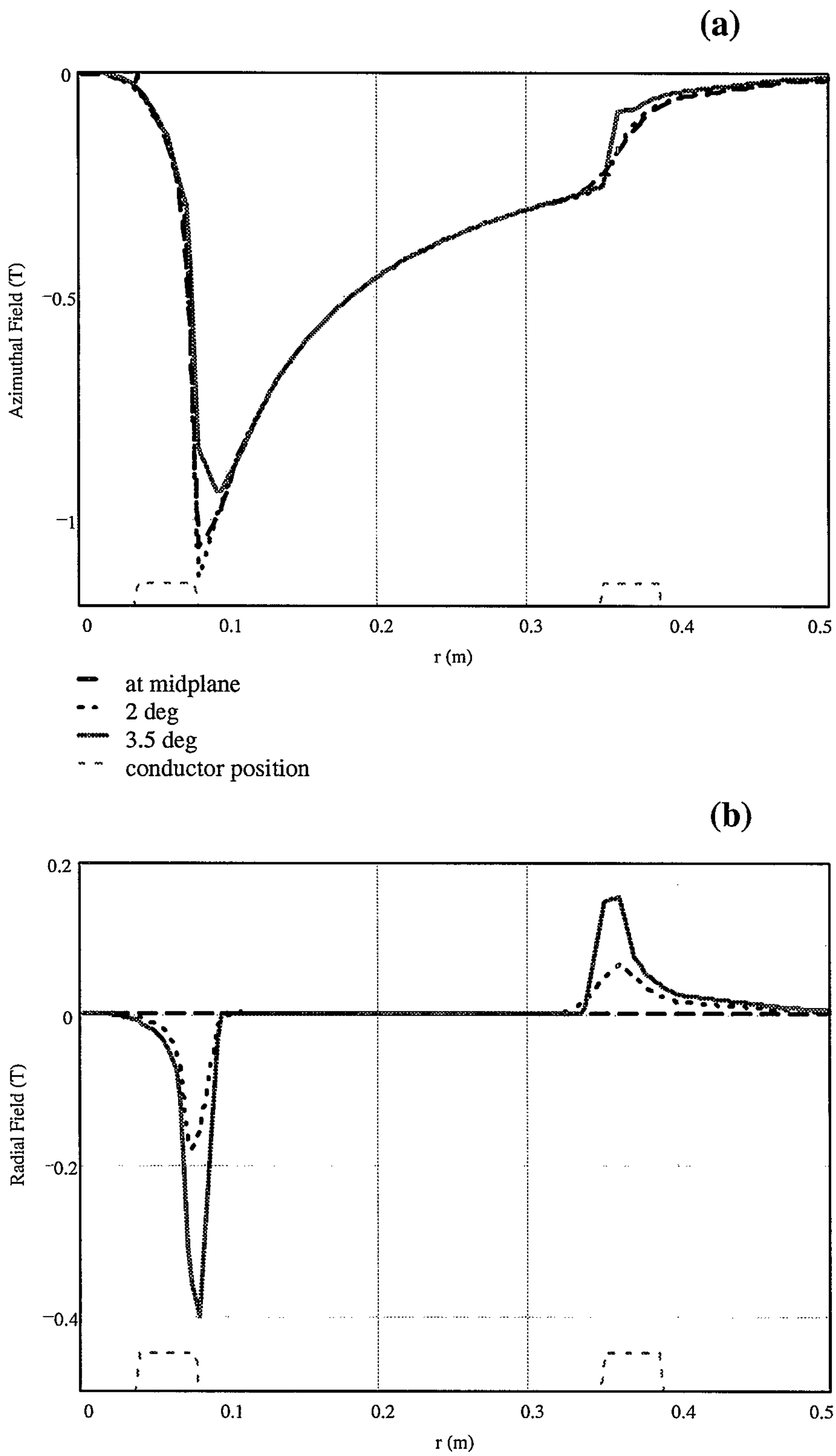


Fig. 3. Toroidal field profiles from TOSCA. The dotted squares near the horizontal axes designate the conductor positions; the radial space between them is iron. Note the substantial radial fields in the vicinity of the conductors. The dotted curve is at $\phi$=2° and the solid curve is at $\phi$=3.5° with respect to the horizontal mid-plane.

pipe in the q4 to q3 region. In order to achieve sufficient field strengths, however, the beam pipe diameter was chosen to be 8 cm.

Figs. 3(a) and (b) show the radial and azimuthal field configurations in the middle of the magnet at a current of about 300 A. The maps plotted are over the upper half of the $7^{\circ}$ opening. Note that there are strong radial fields at the coil positions.

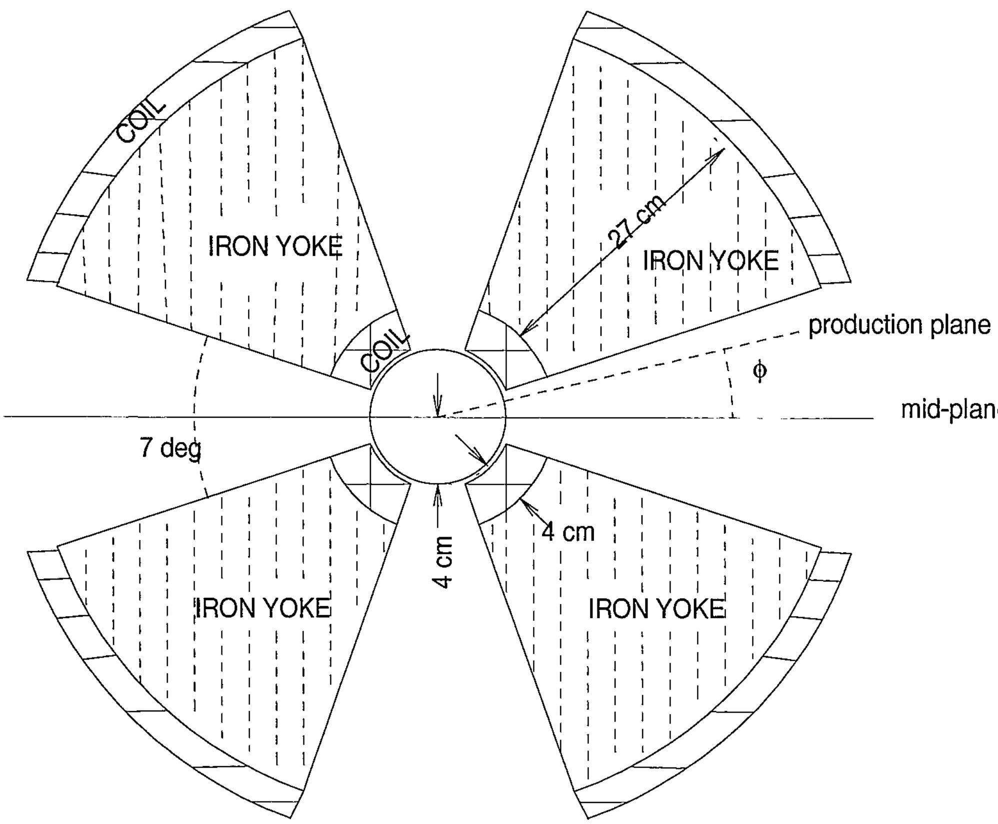


Fig. 2. A sketch of a vertical cut through a toroid magnet. Pions are accepted through the $7^{\circ}$ openings in the horizontal plane. The beam pipe diameter is 8 cm. The inner coil is at $4<r<8$ cm, the iron extends from r=8 to r=35 cm and the outer coil occupies the region $35<r<\sim39$. An arbitrary pion production plane, making an angle $\phi$ with respect to the mid-plane is shown.

| | |
|---|---|
| No. of turns/quadrant | 31 |
| Copper conductor | 9mm X 9mm, 5mm hole |
| Maximum current density | 550 A/cm$^2$ |
| Maximum current | 332 A |
| Voltage | 41 V for $L_{magnet}$=1.5m<br>52 V for $L_{magnet}$=2m |
| Power Supply (bipolar) | 15 KW for $L_{magnet}$=1.5m<br>17 KW for $L_{magnet}$=2m |

Table 1. Parameters of a toroidal magnet design. The voltage specifications were estimated assuming that there will be no fast field ramping requirements.

| | Target | M1 | M2 | M3 | M4 | M5 | M6 | M7 | M8 | Coll. | Crnkv |
|---|---|---|---|---|---|---|---|---|---|---|---|
| **Position (m)** | 1.5 | 2.95 | 5.55 | 7.65 | 9.75 | 11.85 | 13.95 | 16.05 | 18.15 | 20.35 | 25.0 |
| **Length (m)** | 0 | 2 | 1.5 | 1.5 | 1.5 | 1.5 | 1.5 | 1.5 | 1.5 | 4.45 | 6 |
| **Settings@12.5 GeV/c** | | -1 | -1 | -1 | -1 | -1 | -0.5 | +1 | +1 | | |
| **Settings@.50 GeV/c** | | 0 | 0 | -1 | -1 | -1 | +1 | +1 | +1 | | |
| **Settings@87.5 GeV/c** | | 0 | 0 | 0 | -0.5 | -0.3 | +0.5 | +0.95 | +1 | | |
| **Settings@125 GeV/c** | | +1 | +1 | +1 | +1 | +1 | +1 | +1 | +1 | | |

Table 2. Parameters for the layout in fig. 1. The positions of the elements are with respect to the end of q4. The magnet settings are in units of the TOSCA design at about 300A.

The pion production angle $\theta = p_T/p_L$ is the initial pion direction with respect to the beam direction and varies from 64 mrad at $p_{beam}$=25 GeV/c to 6.4 mrad at $p_{beam}$=250 GeV/c. With no special modifications to the 8 cm beam pipe (of assumed wall thickness = 3 mm), pions at the low and high energies will encounter 5 cm and 50 cm of steel resulting in rms scattering angles of 2 mrad and 0.6 mrad, respectively. Together with the expected energy loss, it is likely that this would compromise track reconstruction and momentum resolution. Hence the need for special modifications to the beam pipe whereby exit windows are provided. The engineering details are yet to be addressed and one method is suggested in fig. 1. In this model the beam pipe has sleeves that fit into the magnet gaps.

## 2. Acceptance, Event Rates and Emittance Blowup

Fig. 2 defines $\phi$ as the angle between the magnet mid-plane and the pion production plane. For pions traversing the region of the inner conductor, the $\phi$-acceptance is determined by the strength and direction of the radial fields which are significant only near the conductor positions (see fig. 3(b)). These fields are defocusing in $\phi$ if the polarity of the magnet is set to be radially focusing as is the case for the first 6 magnets in the 12.5 GeV/c case. The position of the first magnet in fig. 1 was chosen such that pions with $p_L$=12.5 GeV/c and $p_T$=0.8 GeV/c do not pass between the inner magnet coils. Instead they enter the first magnet at r>8 cm beyond which the radial fields are insignificant[4]. Fig. 4(a) shows the evolution of the $\phi$-trajectories for the low and high energy cases where it is seen that the acceptance extends nearly to the geometrical aperture limit of $7^{o}$. To illustrate the case, and for comparison, fig. 4(b) shows the $\phi$-acceptance for an earlier layout where the first magnet was placed 0.5 m closer to the target. In this case, the 12.5 GeV/c pions encounter the strong radial fields in the region of the inner coils (r~5 cm) and are consequently defocused away from the mid-plane and the acceptance is limited to about $2^{o}$. The high energy (125 GeV/c) pions, on the other hand, always have full $\phi$-acceptance ($7^{o}$) because the radial fields encountered are always $\phi$-focusing.

[4] This, of course, ignores fringe fields. The effect of fringe fields, which may restrict the acceptance, will be explored at a later time.

A simple estimate of the expected $\theta$-acceptance of the system was made by numerical evaluation of the range of production angles (or $p_T$) that are accepted by the slit collimator. The plots in figs. 5(a) to 5(c) show the acceptance as function of $x_F$ at the 12.5 GeV/c and 125 GeV/c tunes listed in table 2. Even though the kinematic details of the reactions may suppress pion production at high $x_F$ and $p_T$, it is clear that the acceptance remains finite over a long but thin slice of the $x_F$-$p_T$ space - especially at the 125 GeV/c tune. Since the analyzing power depends on $x_F$, the pion momentum must be measured with some accuracy that is yet to be determined.

We follow the detailed calculations of Bunce and Makdisi[5] to get estimates of the event rates and the expected emittance growth. The solid angle is given by,

$$\delta\Omega \approx \delta\theta_h \delta\theta_v \qquad (1)$$

where $\delta\theta_h$ is the $\theta$-acceptance shown in fig.5(c) and,

$$\delta\theta_v \approx 2\tan(\theta_\pi).\sin(\delta\phi). \qquad (2)$$

$\delta\phi$ is the azimuthal acceptance half-angle (~3.2 to 3.5°) and $\theta_\pi \approx \frac{0.8[GeV/c]}{p_L}$ is the production angle. The cross-section may be estimated from

$$\delta\sigma = \left[E\frac{d^3\sigma}{dp^3}\right] p.\delta p.\delta\Omega \qquad (3)$$

where $\left[E\frac{d^3\sigma}{dp^3}\right]$ ~100 μbarns/(GeV/c)$^2$ is the invariant cross-section used by Bunce and Makdisi.

The growth in the normalized emittance due to multiple scattering on the production target (for accumulating $N_\pi$ pions) is given by,

$$\Delta\varepsilon_N\Big|_{95\%} = \frac{3\beta_L}{\beta^3\gamma}\frac{1}{L_{rad}}\left(\frac{0.0141}{0.938}\right)^2\left(\frac{N_\pi}{N_p}\right)\left[\frac{1}{N_A\rho}\right]\left(\frac{1}{\delta\sigma}\right)[\pi] \qquad (4)$$

where, $\beta_L$ is the betatron amplitude at the target position, $\beta$ and $\gamma$ are the usual relativistic factors, $L_{rad}$ and $\rho$ are the radiation length and density of the target material, $N_p$ is the number of protons/fill, $N_A$ is Avogadro's number and $N_\pi$ is the total number of pions accumulated. Note that $\Delta\varepsilon_N$ is independent of the target thickness and the revolution frequency of the beam.

---

[5] Gerry Bunce and Yousef Makdisi, private communications

The event rate $R_\pi$ can be estimated from:

$$R_\pi = d_f^2 \left[ \frac{3\beta\gamma}{\pi\varepsilon_N \beta_L} \right]^{1/2} \left[ f_0 N_p \rho N_A \right] \delta\sigma \qquad (5)$$

where $\varepsilon_N$ is the 95% normalized emittance, $d_f$ is the diameter of the fiber target and $f_0 \approx 80KHz$ is the revolution frequency of the RHIC beam. Table 3 lists estimates of the expected emittance growth and event rates at the 12.5 GeV/c and 125 GeV/c tunes. Several collimator configurations were considered to explore the possibility of enhancing the event rate for the 12.5 GeV/c case.

| **Collimator Parameters** | **$p_\pi$ (GeV/c)** | **$\delta\Omega$ ($\mu$ster)** | **$\delta\sigma$ (nanobarns)** | **$\Delta\varepsilon_N$ ($\pi$.mm.mrad)** | **$N_\pi$/sec** | **$t_\pi$ for $10^4$ $\pi$'s (sec)** | **$N_\pi$/bunch** |
|---|---|---|---|---|---|---|---|
| opening=2cm L=4.45 m | 125 | 0.27 | 42.2 | 0.05 (0.05)** | $9.5*10^4$ | 0.1 | 0.023 |
| opening=2cm L=4.45 m | 12.5 | 4 | 6.3 | 3.1 (3.2)** | 4400 | 2.3 | 0.0011 |
| opening=4cm L=4.45 m | 12.5 | 8.2 | 12.9 | 1.5 | 9100 | 1.1 | 0.0022 |
| opening=2cm L=2 m, slid downstream | 12.5 | 9.9 | 15.4 | 1.3 | $1.1*10^4$ | 0.9 | 0.0026 |
| open=3cm L=2 m, slid downstream | 12.5 | 12.0 | 18.8 | 1.0 | $1.3*10^4$ | 0.8 | 0.0032 |

**Calculated using the graphs in fig. 5(a) and (b), by integrating over $0.45<x_F<0.55$

Table 3. Acceptance and rate estimates for the toroidal polarimeter in fig 1. Also includes expected emittance dilution due to multiple scattering for collecting a total of $10^4$ pions in the two arms of the polarimeter. We used: $\Delta\varepsilon_N = 20$ $\pi$.mm.mrad, protons/fill=52 bunches at$10^{11}$ protons/bunch, carbon fiber diameter = 5 $\mu$m, $p_T = 0.8$ GeV/c, $\delta p/p=0.1$.

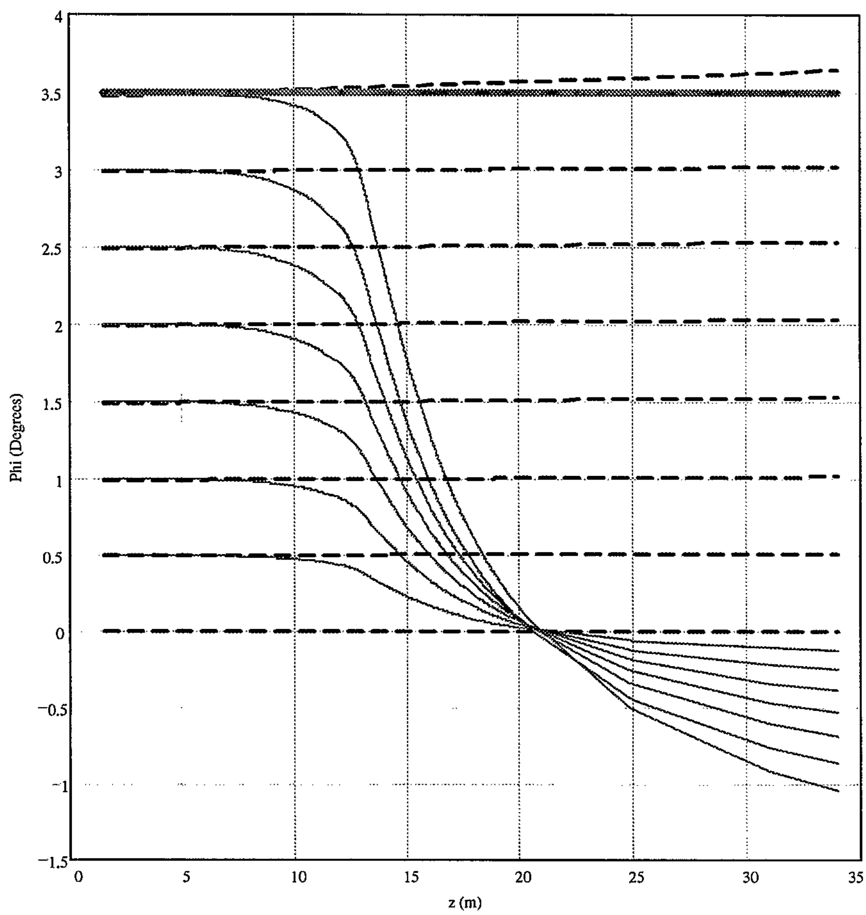


(a)

Fig. 4. The $\phi$ trajectory for various production planes in the upper half of the 7° opening. (a) for the layout in fig 1; for the 12.5 GeV/c case (dashed lines), r~8 cm at the entrance to the first magnet and the acceptance is close to the geometrical limit of 7°. (b) For an earlier layout where r~5 cm at the first magnet; the acceptance is limited to about 2.2°. In both (a) and (b) the field polarity is $\phi$-focusing for the 125 GeV/c pions (solid lines). The physical aperture at 3.5° is shown by the heavy line.

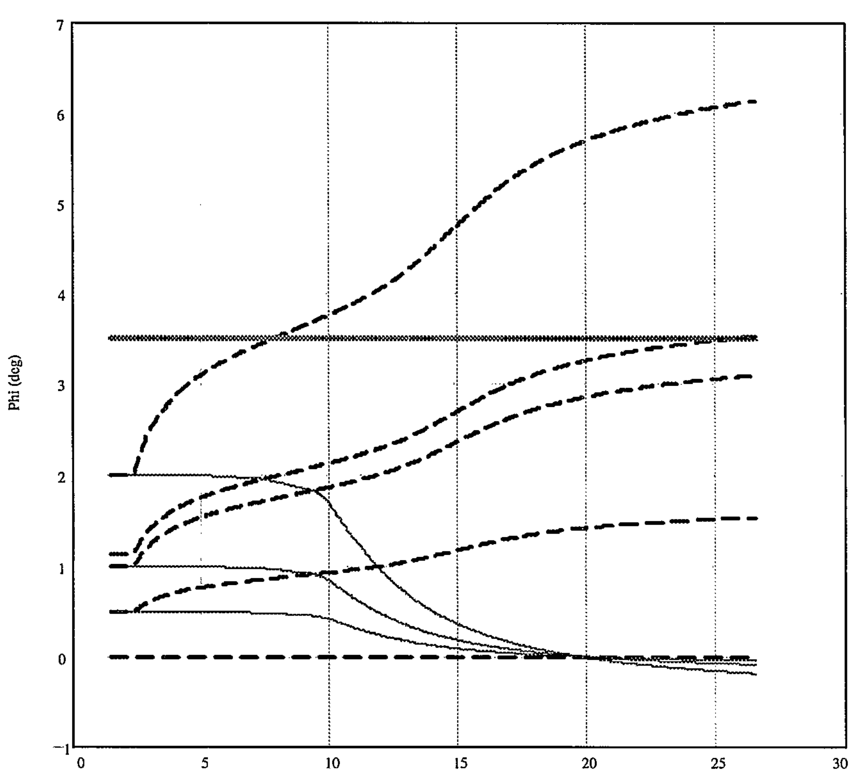


(b)

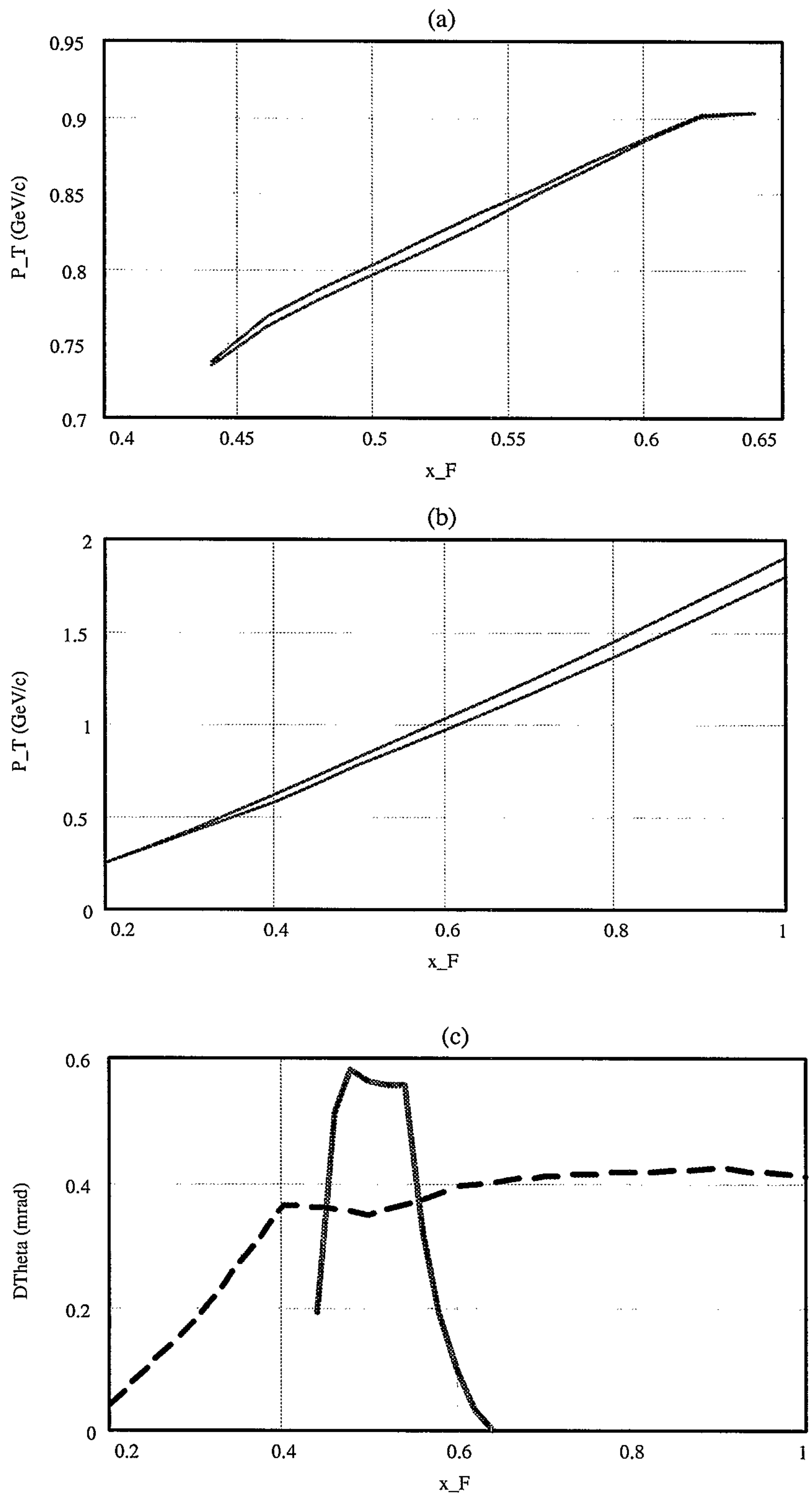


Fig. 5. System acceptance in $x_F$-$p_T$ space for a 4.45 m long collimator with a slit opening of 2 cm. (a) at the 12.5 GeV/c tune, (b) at the 125 GeV/c tune. Acceptance is confined to the region bounded by the two curves. (c) The equivalent geometrical θ-acceptance at the 12.5 GeV/c (solid) and 125 GeV/c (dashed) tunes.

## 3. Summary

The estimates in table 3 indicate that a two-arm pion polarimeter using toroidal magnets may be a viable device for monitoring the polarization of the proton beam at RHIC. Toroids are particularly well suited for this task. Among the most attractive features are: a) The symmetry of the field configuration allows for a symmetric two-arm polarimeter thus making polarization measurements less susceptible to systematic errors. b) Provided the geometrical symmetries of the coil and iron are maintained during production and installation, the symmetry of the field configuration also ensures a zero field region at the beam position. The perturbation to the RHIC beam is thus expected to be minimal and hopefully correctable. c) Toroids produce strong fields close to the production target enabling efficient use of the limited space between q4 and q3. In particular, the simple setup described in this note allows polarization measurements over the entire range of beam momenta from injection to full energy.

The results so far has been encouraging. Nonetheless, further investigations are necessary in order to fully understand some key aspects of the device. Among the most important remaining (and continuing) tasks are:

1. Estimates of background rates, and detector specification need to be addressed and the estimates in table 3 need to be confirmed. This is perhaps best approached using a monte-carlo code which includes the effect of fringe fields. Such a code may also be used to optimize the collimator position and geometry.
2. Issues of compliance with RHIC accelerator specifications will have to be investigated. These include modifications to the beam pipe in order to accommodate exit windows for the pions, and the potentially adverse effects of the toroidal field on the beam.
3. Target mounting and polarimeter operational issues need to be investigated with sufficient detail - especially if they have impact on RHIC operations.
4. Mechanical design of the toroids has already been initiated; alignment and coil placement tolerances need to be specified.
5. A program that can track charged particles through field maps has been developed by Alfredo Luccio. Work is in progress to incorporate this program into a systematic magnet tuning algorithm with parameter optimization capabilities.